SCIENCE CHINA
Physics, Mechanics & Astronomy

• Article •

March 2012 Vol.55 No.3: 514–522
doi: 10.1007/s11433-011-4596-2

# Orbit determination for Chang'E-2 lunar probe and evaluation of lunar gravity models

LI PeiJia[1,2*], HU XiaoGong[1*], HUANG Yong[1*], WANG GuangLi[1], JIANG DongRong[1], ZHANG XiuZhong[1], CAO JianFeng[1,2,3] & XIN Nan[1,2]

[1] *Shanghai Astronomical Observatory, Chinese Academy of Sciences, Shanghai 200030, China;*
[2] *Graduate University of Chinese Academy of Sciences, Beijing 100049, China;*
[3] *Beijing Aerospace Control and Command Center, Beijing 100094, China*

Received September 28, 2011; accepted October 26, 2011; published online February 1, 2012

The Unified S-Band (USB) ranging/Doppler system and the Very Long Baseline Interferometry (VLBI) system as the ground tracking system jointly supported the lunar orbit capture of both Chang'E-2 (CE-2) and Chang'E-1 (CE-1) missions. The tracking system is also responsible for providing precise orbits for scientific data processing. New VLBI equipment and data processing strategies have been proposed based on CE-1 experiences and implemented for CE-2. In this work the role VLBI tracking data played was reassessed through precision orbit determination (POD) experiments for CE-2. Significant improvement in terms of both VLBI delay and delay rate data accuracy was achieved with the noise level of X-band band-width synthesis delay data reaching 0.2–0.3 ns. Short-arc orbit determination experiments showed that the combination of only 15 min's range and VLBI data was able to improve the accuracy of 3 h's orbit using range data only by a 1–1.5 order of magnitude, confirming a similar conclusion for CE-1. Moreover, because of the accuracy improvement, VLBI data was able to contribute to CE-2's long-arc POD especially in the along-track and orbital normal directions. Orbital accuracy was assessed through the orbital overlapping analysis (2 h arc overlapping for 18 h POD arc). Compared with about 100 m position error of CE-1's 200 km×200 km lunar orbit, for CE-2's 100 km×100 km lunar orbit, the position errors were better than 31 and 6 m in the radial direction, and for CE-2's 15 km×100 km orbit, the position errors were better than 45 and 12 m in the radial direction. In addition, in trying to analyze the Delta Differential One-Way Ranging (ΔDOR) experiments data we concluded that the accuracy of ΔDOR delay was dramatically improved with the noise level better than 0.1 ns and systematic errors better calibrated, and the Short-arc POD tests with ΔDOR data showed excellent results. Although unable to support the development of an independent lunar gravity model, the tracking data of CE-2 provided evaluations of different lunar gravity models through POD. It is found that for the 100 km×100 km lunar orbit, with a degree and order expansion up to 165, JPL's gravity model LP165P did not show noticeable improvement over Japan's SGM series models (100×100), but for the 15 km×100 km lunar orbit, a higher degree-order model can significantly improve the orbit accuracy.

**Chang'E-2, VLBI, orbit determination, lunar gravity field**

**PACS number(s):** 95.10.Eg, 95.40.+s, 95.55.Pe, 95.75.Kk ,96.20.Jz

**Citation:** Li P J, Hu X G, Huang Y, et al. Orbit determination for Chang'E-2 lunar probe and evaluation of lunar gravity models. Sci China-Phys Mech Astron, 2012, 55: 514–522, doi: 10.1007/s11433-011-4596-2

The Chang'E-2 (CE-2) probe was launched on October 1, 2010. After nearly 5 d trans-lunar journey, it was captured by the Moon on October 6, 2010, and then successfully became a lunar satellite on a polar, near circular orbit with an altitude of approximately 100 km. On October 26, 2010, CE-2 descended to 15 km to obtain photographs of the Sinus Iridum area. CE-2 is the second lunar probe of China. Compared to Chang'E-1 (CE-1) it was directly injected into

*Corresponding author (email: LI PeiJia: pjli@shao.ac.cn; HU XiaoGong: hxg@shao.edu.cn; HUANG Yong: yongh@shao.ac.cn)

the trans-lunar orbit with the objectives to demonstrate key technologies for lunar landing, such as X-band tracking and control, high resolution imaging and so on. Useful methodology and software was developed for the mission and practical experience in engineering was accumulated, which benefits the follow-on deep space explorations of China.

Both the Unified S-Band (USB) range/Doppler system and Very Long Baseline Interferometry (VLBI) system were used in CE-1 and CE-2 missions. Since the VLBI technology is able to provide high accuracy observations through differential interferometry and has no demand for up-link transmission, it is a helpful supplement to radio range/Doppler measurements. During the last 5 years, Chinese VLBI Network (CVN) has accumulated artificial spacecraft tracking experience for both Earth observation satellites and deep space exploration spacecrafts, such as TanCe-1 [1], COMPASS navigation satellites [2], CE-1 [3], SMART-1 and Mars Express [4].

In the CE-2 mission, one of the important improvements of VLBI system was using the Digital Base-Band Converter (DBBC) in place of the Analog Base-Band Converter (ABBC) used in the CE-1 mission. Shanghai Astronomical Observatory (SHAO) [5] started to develop DBBC a few years before hoping to overcome the non-linear phase-frequency response of ABBC for better accuracy. After numerous experiments and observational trials, DBBC was proved to satisfy design requirements and successfully applied in the CE-2 mission.

Post-processing strategies of the VLBI system were also improved. During the CE-1 and CE-2 missions, two observation modes were available [6]: real-time mode and post-processing mode. For the real-time mode, VLBI observations were processed in less than 5 min after the reception of the 500 kHz bandwidth S-band signals. In this mode, the observations of extragalactic radio sources (i.e., quasars) before the satellite tracking arcs were used to correct systemic errors such as receiver delay, clock offset and drifts. The quasar observations last about 1 or 2 h while satellite tracking arcs could be from 8 to 12 h; hence significant time varying systemic errors remained and deteriorated the orbit determination accuracy [7]. As an improvement, in the CE-2 mission, in conjunction with quasars, long time series (from 5 to 7 d) of GPS data were also used to correct the VLBI station clock drifts, and resulting in more precise estimates of the systemic errors thanks to the stability of the GPS time series. Different from the real-time mode, in the post-processing mode, quasar observations both before and after satellite tracking arcs were used to correct the clock drift, which could help to achieve higher accuracy of VLBI data. Furthermore, nearly 50% post-processing mode data of CE-2 was obtained with the bandwidth synthesis technique, which used 20 MHz bandwidth X-band signals and the delay data noise level reached 0.2 ns.

The Delta Differential One-Way Ranging (ΔDOR) tracking technology is recommended in deep space explorations with the advantages of low transmitting energy demand on-board and simple processing system on the ground. In the CE-2 mission, X-band tracking and control experiments were implemented and the ΔDOR data was provided by the VLBI system [8].

The altitude of CE-1's nominal lunar orbit was about 200 km; however, in the CE-2 mission the altitude was lowered to about 100 km for better image resolution, and it even descended to 15 km to complete the close-up imaging task for Sinus Iridum area during October 26–29, 2010. As the altitude dropped, the orbital perturbation of lunar gravity on the satellite increased, and the precision orbit determination (POD) accuracy of lunar orbit satellite is limited by the accuracy and resolution of the lunar gravity model. As an independent data set, the tracking data of CE-2 was unable to support the development of an independent lunar gravity model; however, it can provide useful evaluations on different lunar gravity models through POD.

In this paper, POD of CE-2 on various lunar orbits is studied using different tracking data combinations, with an emphasis on contributions of the improved VLBI tracking data. The ΔDOR data of the X-band tracking and control system experiments are also analyzed. Performance of different gravity field models is discussed through POD. Orbit determinations are processed with a specifically modified version of GEODYNII [9]. This paper is structured as follows. The VLBI data improvements and the results for orbit determination of the CE-2 satellite are described in sect. 1. The analysis of X-band tracking experiment is presented in sect. 2. The evaluation of different gravity field models is described in sect. 3, and conclusions follow in sect. 4.

## 1 POD of CE-2: analysis and discussion

According to the principle of VLBI, the time delay between the arrivals of the same wave-front at two antennae (the delay $\tau$) and the temporal rate of the change of the time delay (the delay rate $\dot{\tau}$) are measured via radio signal interference. As we know, VLBI technology is able to obtain extremely high accurate observations, and different from most range/Doppler tracking systems, uplink transmission is not necessary. Furthermore, weak signal very far away is picked up with large antennas. For the above reasons, VLBI is a useful supplement to usual radio range and velocity measurement techniques and can be applied in lunar and deep space explorations. Simulation results show that joint orbit determination using VLBI and range/Doppler data can improve the POD accuracy [9–11]. The formulations of VLBI measurements are given as follows, for VLBI delay,

$$\tau = \frac{1}{c}(\rho_1 - \rho_2) = \frac{1}{c}\left(\left|\boldsymbol{r}(t) - \boldsymbol{R}_1(t_2)\right| - \left|\boldsymbol{r}(t) - \boldsymbol{R}_2(t_2)\right|\right), \quad (1)$$

for VLBI delay-rate,

$$\dot{\tau} = \frac{1}{c}(\dot{\rho}_1 - \dot{\rho}_2) = \frac{1}{c}\left(\frac{(\boldsymbol{r}(t)-\boldsymbol{R}_1(t_1))\cdot(\dot{\boldsymbol{r}}(t)-\dot{\boldsymbol{R}}_1(t_1))}{\rho_1} - \frac{(\boldsymbol{r}(t)-\boldsymbol{R}_2(t_2))\cdot(\dot{\boldsymbol{r}}(t)-\dot{\boldsymbol{R}}_2(t_2))}{\rho_2}\right), \quad (2)$$

where $\boldsymbol{r}(t)$ is the probe position at the signal transmission moment, $\boldsymbol{R}_1(t_1)$ is the station 1 position at the moment when signals arrived at station 1, and $\boldsymbol{R}_2(t_2)$ is the station 2 position at the moment when signals arrived at station 2.

According to different observation modes and processing methods, four kinds of VLBI data existed in the CE-2 mission: (1) S-band data in real-time mode. The delay data noise level is about 1–1.5 ns. (2) S-band data in post- processing mode. The delay data noise is equivalent to the real time, but the systematic errors are improved. (3) X-band bandwidth synthesis data in post-processing mode. The delay data noise level can reach 0.2–0.3 ns. (4) ΔDOR data in X-band tracking and control experiments. The ΔDOR delay data noise level can reach 0.1 ns. In addition, compared with the first three types of delay-rate data, whose noise level is about 0.2–0.3 ps/s, the ΔDOD shows noticeable improvement.

The POD accuracy was directly influenced by the accuracy of the tracking data. In this section, CE-2's lunar orbit accuracy and contributions of VLBI are assessed by means of tracking data residuals analysis, short arc POD analysis and orbital overlap statistics. The range and Doppler data were sampled every 1 s, whereas the delay and delay rate data were provided every 5 s on all baselines. Because of pre-processing flaws with the Doppler data, only range and VLBI data were calculated. According to the experience accumulated in CE-1, the range, delay and delay-rate data were weighted with a standard deviation ($\sigma$) of 3 m, 1 m and 0.01 cm/s, respectively.

### 1.1 Residuals analysis

During the course of the mission, CE-2 is commanded to perform orbital correction maneuvers, reorientation maneuvers, trimmed its spin rate and so on. As far as the POD study is concerned, all the forces acting on the spacecraft should be modeled accurately to recover the orbit. However, since the modeling of these maneuvers are difficult and the results are not positive enough [12], the arcs including orbital maneuvers are avoided in POD experiments. Instead, these arcs are divided into two arcs with one priori to a maneuver and one after the maneuver.

In order to assess the accuracy of various tracking data types, post-fitting residual root-mean-square (RMS) summary for CE-1 and CE-2 is shown in Table 1. It is found that compared with CE-1, the residual RMS of CE-2 data for both the real-time mode and the post-processing mode were significantly improved, especially for the X-band bandwidth synthesis data, the delay data residual of which was reduced to 1–2 ns. During CE-2's lunar orbit, the noise level of VLBI data is stable, and it is about 1.5 ns for the S-band delay data and 0.3 ns for X-band bandwidth synthesis data with a better corrected systematic bias. Figure 1 shows a sample of time series of residual delay and delay-rate plots for CE-2.

### 1.2 Short-arc orbit determination (SOD)

Spacecraft is often designed to carry out certain experiments on different orbits; for that reason, it is necessary to perform orbit maneuver to change its altitude. Additionally, because the lunar gravity field has a strong effect on the evolution of

**Table 1** Solution residual RMS summary for CE-1 and CE-2

| | Data type | | Delay (ns) | Delay-rate (ps/s) |
|---|---|---|---|---|
| CE-1 | Post-processing: S-band | | 6.15 | 0.70 |
| CE-2 | Real-time: S-band | | 4.93 | 0.64 |
| | Post-processing | S-band | 4.04 | 0.63 |
| | | bandwidth synthesis | 1.28 | 0.45 |

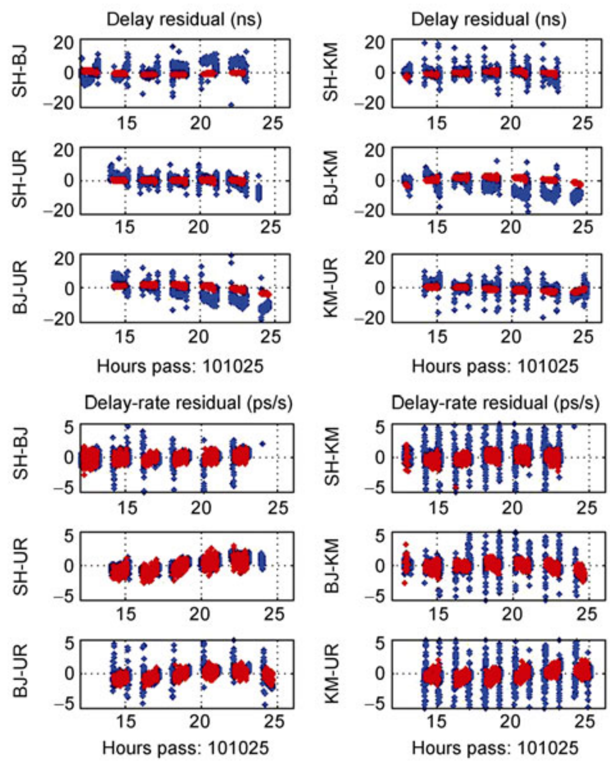


**Figure 1** VLBI data residual time series on October 25, 2010 (blue for S-band data in the real-time mode, red for X-band bandwidth synthesis data; BJ, SH, KM, UR represent Beijing, Shanghai, Kunming and Urumqi, respectively).

a low altitude orbit [13], orbit maintenance maneuvers are required in order to keep the spacecraft within a desired altitude range.

After an orbital maneuver, rapid orbital recovery, or SOD is crucial for tracking and control system to assess the maneuver performance. VLBI data was demonstrated to make enormous contributions to the SOD in the CE-1 mission. Calculations showed that the combination of only 30 min' range and VLBI data was able to improve the orbit accuracy better than using 3 h's range data alone. In this section, SOD accuracy of CE-2 was investigated to evaluate the contributions of the improved VLBI data. Considering SOD was necessary in real-time tasks, only the S-band real-time mode data was applied.

Taking the POD results which combine 18 h long-arc range and post-processing VLBI data as precise ephemeris, and using 15 min's, 30 min's and 3 h's range and VLBI data to determine the orbit respectively, RMS position difference between precise ephemeris and SOD ephemeris, as well as, between precise ephemeris and 3 h prediction ephemeris of SOD (3 h-Pre) were calculated and the results are shown in Table 2. The analysis indicates: (1) SOD using only 15 or 30 min's range data may not result in convergent orbits until probably 3 h's range data is collected, and the convergent orbits are possible with the position error being about 1.2 km; (2) combining VLBI data can improve the stability and accuracy of SOD. Table 2 shows the position accuracy of 15 min's combined SOD is better than 65 m, which is a 1–1.5 order of magnitude improvement relative to the 3 h's range data only results; (3) with an orbital period of about 2 h, when the SOD arc lengths are as long as 3 h, the orbital prediction errors are equivalent to the SOD errors. However, for 15 or 30 min SOD arc, the prediction errors are as large as about 500 m.

### 1.3 Overlapping analysis

The orbit determination errors can be accessed by looking at the overlapping differences between arcs. Since the orbit period was about 2 h, the POD arcs were chosen to be 18 h with 2 h overlapping, and the maneuver event arcs were avoided. For each POD arc, the spacecraft position, velocity, range biases and solar radiation coefficient are estimated, and the gravity field model used is LP165P [14] unless indicated otherwise.

The orbital overlapping results of CE-2's 100 km× 100 km orbits (or the altitude of 100 km) are shown in Table 3. The AEN (Angle between the Earth-Moon vector and

**Table 2** Results of SOD using various combinations of the tracking data

| Orbit arc | RMS of position differences (m) | | | | | |
|---|---|---|---|---|---|---|
| | 15 min | | 30 min | | 3 h | |
| | SOD | 3 h-Pre | SOD | 3 h-Pre | SOD | 3 h-Pre |
| VLBI+range | 61.67 | 544.50 | 36.06 | 496.67 | 18.55 | 19.31 |
| Range | No convergence | | No convergence | | 1239.36 | 1233.86 |

**Table 3** RMS of orbital overlapping errors for CE-2's 100 km×100 km orbit using various combinations of the tracking data (*R*, *T* and *N* signify radial, transverse and normal directions, respectively. 12d02h/12d04h represents the overlapping arc of two POD arcs: one is from 2010-10-11T10:00:00 to 2010-10-12T04:00:00, and the other is from 2010-10-12T02:00:00 to 2010-10-12T20:00:00, with 2 h overlapping arcs)

| Overlapping arc | Data used for POD | *R* (m) | *T* (m) | *N* (m) | Total (m) | AEN (°) |
|---|---|---|---|---|---|---|
| 12d18h/12d20h | range | 9.59 | 59.93 | 199.43 | 208.46 | 80.29 |
| | range+VLBI | 8.23 | 16.97 | 26.36 | 32.41 | |
| 13d10h/13d12h | range | 3.72 | 66.68 | 145.62 | 160.21 | 71.64 |
| | range+VLBI | 5.01 | 12.90 | 10.14 | 17.16 | |
| 14d02h/14d04h | range | 1.66 | 120.35 | 173.57 | 211.22 | 63.27 |
| | range+VLBI | 5.33 | 13.17 | 19.21 | 23.89 | |
| 20d04h/20d06h | range | 14.66 | 37.67 | 4.98 | 40.73 | 11.64 |
| | range+VLBI | 8.10 | 20.19 | 2.52 | 21.90 | |
| 20d20h/20d22h | range | 7.32 | 53.02 | 13.46 | 55.19 | 19.03 |
| | range+VLBI | 6.55 | 42.72 | 10.45 | 44.47 | |
| 24d06h/24d08h | range | 6.56 | 76.86 | 102.58 | 128.35 | 60.19 |
| | range+VLBI | 2.26 | 22.54 | 30.36 | 37.88 | |
| 24d22h/25d00h | range | 6.62 | 122.77 | 210.12 | 243.45 | 68.55 |
| | range+VLBI | 3.26 | 6.83 | 13.61 | 15.57 | |
| Average | range | 6.48 | 63.24 | 97.32 | 122.72 | – |
| | range+VLBI | 5.38 | 21.59 | 16.24 | 30.76 | |

the Nominal vector of the orbital plane) of overlapping arcs 20d04h/20d06h, and 20d20h/20d22h is less than 20°, which is about the same view geometry as the face-on view geometry where the normal vector of the orbital plane is perpendicular to the Earth-Moon vector. From Table 3, it is obvious that when the AEN is less than 20°, compared with the POD result with range data only, VLBI data contribute less, but for other view geometries, it improves the orbit overlapping to a great extent, especially in the along-track and orbital normal directions. It is because during the near face-on view geometry, using range data alone can already reach a desirable accuracy. The radial average error is better than 6 m, and the total difference is improved from 123 to 31 m.

Table 4 shows the overlapping differences for 15 km×100 km lunar orbit. The order of magnitude improvement is made possible by the VLBI data: the radial average error is better than 12 m, and the total differences are improved from 530 to 45 m.

The POD accuracy of CE-1's 200 km×200 km orbit was estimated to be about 100 m [15,16] and less than 10 m in the radial on average. For other lunar explorations, both LP [17] and SELENE [18] have the same orbital altitude with CE-2; however, orbital overlapping experiments showed the RMS position difference was about 10 m for LP [19], and 20 m for SELENE [20,21]. Compared with CE-1, although the same tracking system and network was used in CE-2, the POD result was significantly improved by the high quality VLBI data. When it comes to LP and SELENE, the POD accuracy differences were mostly due to the tracking system. LP was tracked by three 26 m antennae and six 34 m antennae of DSN/JPL with a range noise level better than 0.1 m, and for SELENE, apart from the four-way Doppler tracking system, it was tracked by VERA (composed of 4 VLBI stations of Japan) and other 4 international VLBI stations with the same-beam differential VLBI data [22], which reached higher accuracy than CVN. However, for CE projects, the range noise level was about 1 m and only 4 domestic VLBI stations provided less than 10 h observations each day. With the construction of Chinese deep space network and further improvement of CVN, more accurate orbits and scientific data can be obtained, which will contribute to follow-on Chinese deep space projects.

## 2 ΔDOR data analysis

The practice of ΔDOR tracking is to precisely measure station-wise difference in both the target tracked and a reference quasar's signal phases, and then difference the extragalactic radio source and the target's station-wise differences to arrive at quasar-target station-wise double difference. Given the high precision of quasar location on the celestial plane, the purpose of the double differencing is to remove systemic errors originating from both station devices and atmospheric effects. In principle, ΔDOR is the target-quasar differential of VLBI delay; and its time derivative, ΔDOD is the target-quasar differential of VLBI delay rate. Usually a ΔDOR tracking session consists of three observation parts: an observation sub-session of a nearby radio sources is followed by a sub-session of target observation, and then to another sub-session of nearby radio source, with each part lasting about a few minutes for optimal systemic error correction. When the radio source and the target are on the same line-of-sight direction, ΔDOR and ΔDOD measurements are able to eliminate almost all the common error sources, such as ionosphere refraction delay, troposphere refraction delay, site coordinate errors, etc., and in consequence, the accuracy was significantly improved.

During the CE-2 mission 5 ΔDOR experiments were planned and successfully carried out in October, 2010, and in April, 2011, there were 17 consecutive ΔDOR experiments. This section takes the experiment on October 3, 2010 as an example and analyzes the ΔDOR experimental data through orbit determination.

The orbital type of this experiment was trans-lunar orbit, and the arc length of ΔDOR experiment was about 4 h. In order to assess the accuracy of the ΔDOR data, the S-band post-possessing mode VLBI data and the ΔDOR data were

**Table 4** RMS of orbital overlapping errors for the 15 km×100 km orbit using various combinations of the tracking data (*R*, *T* and *N* signify radial, transverse and normal directions, respectively. 27d09h/27d11h represents the overlapping arc of two POD arcs: one is from 2010-10-26T17:00:00 to 2010-10-27T11:00:00, and the other is from 2010-10-27T09:00:00 to 2010-10-28T03:00:00, with 2 h overlapping arcs)

| Overlapping arc | Data used for POD | *R* (m) | *T* (m) | *N* (m) | Total (m) | AEN (°) |
|---|---|---|---|---|---|---|
| 27d09h/27d11h | range | 5.50 | 90.96 | 434.74 | 444.19 | 104.29 |
| | range+VLBI | 12.85 | 30.74 | 40.53 | 52.47 | |
| 28d00h/28d02h | range | 6.46 | 340.94 | 875.22 | 939.30 | 104.50 |
| | range+VLBI | 10.56 | 31.73 | 13.28 | 35.98 | |
| 28d16h/28d18h | range | 18.24 | 87.18 | 164.07 | 186.69 | 121.16 |
| | range+VLBI | 11.76 | 24.23 | 40.64 | 48.75 | |
| Average | range | 10.07 | 173.03 | 491.34 | 523.39 | – |
| | range+VLBI | 11.72 | 28.90 | 31.48 | 45.73 | |

processed respectively. Calculations showed the residual RMS of ΔDOR data was better than 0.42 ns and the ΔDOD was about 0.21 ps/s, both of which were largely improved compared with the S-band VLBI data, which was about 3.41 ns (delay data) and 0.40 ps/s (delay-rate data), respectively. Figure 2 shows the OD residual time series plots of the experiment on October 3, 2010 (blue for S-band data in the real-time mode, red for X-band ΔDOR and ΔDOD experimental data). It is found that the S-band delay data noise is about 1–2 ns, whereas the ΔDOR noise level can be better than 0.1 ns. Moreover, for S-band delay data, 3 ns systematic bias exists in baselines related to SH station. During the last half part of this experiment, baselines related to UR station reveal a changing systematic bias, which was up to 7 ns. In contrast, the residuals of ΔDOR data are smooth for all baselines, since the ΔDOR measurements are able to eliminate almost all the common error sources, and the systematic bias problems are well corrected.

The residuals analysis above indicates that the accuracy of ΔDOR experimental data is significantly improved over the traditional VLBI data. However, since ΔDOR experiments arcs are not long enough to carry out long-arc POD analysis for the trans-lunar orbit, this section only investigated SOD with ΔDOR data. Taking the POD result using 18 h's range and post-processing mode VLBI data as precise ephemeris, the accuracy of which was about 30 m (sect. 1.3), RMS of position difference between precise ephemeris and 15 min SOD results with different data types is shown in Table 5.

As the CE-2 flying farther away from the Earth, dynamic constraints on it become weaker. For that reason, POD errors using 12 h range data respectively was worse than 300 km compared with the precise ephemeris. However, combing S-band VLBI and range data with 15 min length arcs is able to reduce orbit errors to about 250 m; furthermore, using ΔDOR and range data with 15 min length arcs is able to improve the accuracy to be better than 140 m.

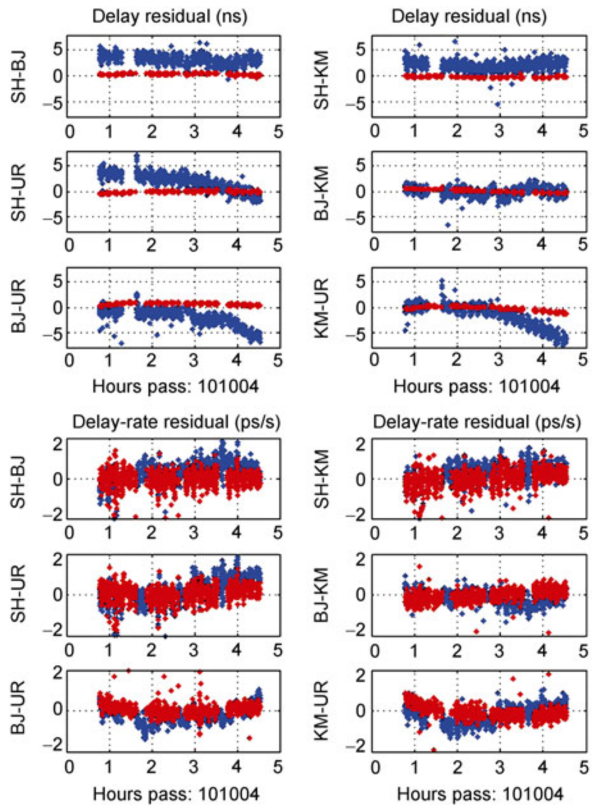


**Figure 2** VLBI data residual on October 3, 2010 (blue for S-band data in the real-time mode, red for X-band ΔDOR & ΔDOD experimental data; BJ, SH, KM, UR represent Beijing, Shanghai, Kunming and Urumqi, respectively).

## 3 Evaluation of different lunar gravity models

The precision of lunar satellite orbit determination depends on the quality of the lunar gravity field model, since gravity is the dominating perturbing force acting on the satellite. The study of lunar gravity field began in 1966 with the Lunar 10 mission of Russia, which provided the dynamical proof that the oblateness of the Moon was larger than the

**Table 5** Ephemeris differences for 15 min SOD using various combinations of the tracking data

| | Data used for SOD | *R* (m) | *T* (m) | *N* (m) | Total (m) |
|---|---|---|---|---|---|
| 1 | ΔDOR + range | 43.17 | 114.96 | 35.79 | 127.91 |
| | VLBI + range | 38.76 | 15.10 | 302.36 | 305.20 |
| 2 | ΔDOR + range | 20.84 | 98.59 | 90.87 | 135.69 |
| | VLBI + range | 15.55 | 17.49 | 412.42 | 413.09 |
| 3 | ΔDOR + range | 21.29 | 93.51 | 96.75 | 136.22 |
| | VLBI + range | 18.70 | 15.15 | 265.35 | 266.44 |
| 4 | ΔDOR + range | 21.82 | 92.14 | 98.82 | 136.86 |
| | VLBI + range | 19.01 | 44.11 | 279.39 | 283.49 |
| 5 | ΔDOR + range | 22.28 | 89.47 | 104.04 | 139.01 |
| | VLBI + range | 19.99 | 57.82 | 248.22 | 255.65 |
| Average | ΔDOR + range | 25.88 | 97.73 | 85.25 | 135.14 |
| | VLBI + range | 22.402 | 29.93 | 301.55 | 304.77 |

shape predicted from hydrostatic equilibrium. After that, Muller and Sjogren [23] differentiated the Doppler residuals of Lunar Orbiter (LO)-V, and provided a nearside gravity map and discovered the mascons in the lunar interior. The subsequent missions of LO and Apollo 15 and Apollo 16 contributed a lot to the early research of lunar gravity field.

In 1994, Clementine spacecraft was lunched, and the laser-ranging measurements provided the first view of the global topographic figure of the Moon [24]. Lemoine [25] developed the GLGM-2 lunar gravity model using the Clementine tracking data with the historic lunar orbiter and Apollo data. Because the Clementine was working on an elliptical orbit with a 400 km periapse altitude, the GLGM-2 model improved the low degree and sectoral terms of the lunar gravity field.

The lunar Prospector (LP) spacecraft was launched in 1998, and its objectives were to generate a global compositional map of the lunar surface and update the knowledge of the lunar magnetic and gravity fields [17]. It was the first time to obtain the measurements on a low polar circular orbit with a complete coverage at a high resolution for the entire lunar nearside. Based on the tracking data of LP, Konopliv et al. [14,26] developed a series of lunar gravity models. Among them, the LP165P model used historic lunar satellite data with all the LP nominal and extended mission data (the lowest altitude was less than 10 km), which is the highest degree lunar gravity model till now.

The Moon's rotation is synchronized to its orbital revolution. As a result, only one side of the Moon can be directly seen from the Earth, and therefore, the lunar farside gravity field is poorly determined. The Japanese SELENE mission with a satellite-to-satellite Doppler tracking subsystem [18] was launched on September 14, 2007. In this mission the four-way Doppler measurement (Earth antenna -> sub-satellite-> main-satellite-> sub-satellite-> Earth antenna) helped to obtain the tracking data of the main-satellite over the farside. Japanese scientists using the SELENE data [27] developed a series of SGM (SELENE Gravity Model) lunar gravity fields, which were the first models using the farside tracking data.

Yan et al. [28] combined CE-1 tracking data with orbital tracking data of SELENE, LP and historical spacecrafts, developed a high accuracy lunar gravity field model CEGM02, and found that CE-1 orbital tracking data is able to contribute to long wavelength of lunar gravity field.

Both the LP165P model and the SGM models have their own advantages. The former integrated the extended mission data of LP, and had higher degree and order, while the SGM models included the direct tracking data of the Moon's farside. The SGM100i model included VLBI data while the SGM100h model did not.

In this section, since the tracking data of the CE-2's lunar orbits (100 km×100 km and 15 km×100 km) is independent of the lunar gravity models mentioned above, it can evaluate the accuracy of different lunar gravity models through POD. The gravity models used are LP165P (165×165), LP165P (100×100), SGM100i and SGM100h.

### 3.1 100 km×100 km orbit

As mentioned in the introduction, avoiding the orbit maneuver arcs, the POD of CE-2 was based on range and VLBI delay and delay-rate data. Overlapping analysis results for 100 km× 100 km orbit were summarized in Table 6. It is found that the orbit errors are nearly the same using LP165P (165×165), LP165P (100×100), SGM100h and SGM100i models, and the position errors were about from 30 to 35 m, while the POD accuracy using SGM100h models is slightly lower and the position errors was up to 54 m.

For a better understanding of how well the gravity field predicts the orbit of CE-2 over a long time, we used POD solution to predict 18, 36 and 54 h, respectively and compared the prediction results with POD solution. This was done during the arcs where no spacecraft maneuvers were performed and the length for POD arc was 18 h. Figure 3 shows the differences with POD solutions for the four gravity fields LP165P (165×165), LP165P (100×100), SGM100i and SGM100h. It is found that the propagation accuracy of SGM100i was higher than that of the other three models and the position error of 54 h's propagation was less than 100 m.

From the analysis above, it can concluded that 100 degree gravity models is enough for 100 km×100 km lunar orbit POD, and the SGM100i model which includes VLBI data performed better POD and propagation accuracy compared with other models.

### 3.2 15 km×100 km orbit

Overlapping analysis results for the 15 km×100 km orbit were summarized in Table 7. Because the continuous

**Table 6** RMS of orbital overlap errors of different lunar gravity models for the 100 km×100 km lunar orbit

| Gravity models | *R* (m) | *T* (m) | *N* (m) | Total (m) |
|---|---|---|---|---|
| LP165P(165) | 5.38 | 21.59 | 16.24 | 30.76 |
| LP165P(100) | 6.09 | 22.48 | 17.39 | 32.53 |
| SGM100i | 6.71 | 27.36 | 16.45 | 35.70 |
| SGM100h | 13.07 | 40.06 | 26.20 | 53.65 |

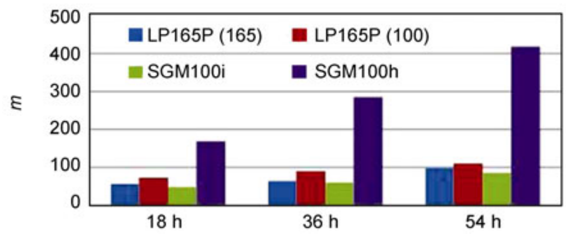


**Figure 3** RMS of orbital propagation errors with different lunar gravity models for the 100 km×100 km lunar orbit.

**Table 7** RMS of orbital overlap errors of different lunar gravity models for the 100 km×100 km lunar orbit

| Gravity models | *R* (m) | *T* (m) | *N* (m) | Total (m) |
|---|---|---|---|---|
| LP165P(165) | 11.72 | 28.90 | 31.48 | 44.31 |
| LP165P(100) | 38.10 | 85.28 | 58.63 | 110.28 |
| SGM100i | 41.60 | 72.35 | 52.24 | 98.46 |
| SGM100h | 53.24 | 118.12 | 61.49 | 143.41 |

maneuver-free arcs were not long enough on the 15 km×100 km orbit, the propagation error analysis was not performed. The experiments show that the high degree-order gravity field model (165×165) performs much better than 100 degree-order gravity models in terms of POD accuracy for 15 km×100 km. For the LP165P models, the position errors were better than 45 m (12 m in radial), whereas for the other three models, the position errors was about from 98 to 143 m. Again, the SGM100i model provided better accuracy than the other models with 100 degree-order resolution.

## 4 Conclusions

New VLBI equipment and data processing strategies brought significant improvements in data accuracy for the CE-2 mission. In this paper, residual RMS for CE-2 and CE-1 data were calculated. The results indicated that compared with CE-1 data, both the real-time mode and the post-processing mode data of CE-2 were significantly improved, especially for the X-band bandwidth synthesis data, the delay data residual of which was reduced to 1–2 ns and the noise level can be better than 0.3 ns. The systematic bias problems were better corrected.

In the CE-1 mission, VLBI data was proved to bring enormous contribution to the SOD. Given the improvement of the CE-2 data, we investigated the SOD and found that the combination of only 15 min's range and VLBI data is able to improve the orbit accuracy by a 1–1.5 order of magnitude with respect to 3 h's range data alone.

Furthermore, orbital overlapping (2 h arc overlapping for 18 h POD arc) analysis indicates that when the viewing geometry is not face-on, VLBI data is able to largely improve the POD accuracy, especially in the *T* and *N* directions. For the 100 km×100 km lunar orbit, the position errors are better than 30 and 6 m in the radial direction, and for the 15 km×100 km orbit, the position errors are better than 45 and 12 m in the radial direction. Compared with CE-1's POD results, CE-2 shows a higher accuracy because of the improvement of VLBI data accuracy.

In sect. 2, ΔDOR experiments data is processed, and the results show that compared with the noise level of S-band VLBI delay data, which is about 1–2 ns, the noise level can be better than 0.1 ns for ΔDOR data and the systematic bias problems are well corrected. Furthermore, the residual RMS of ΔDOR data is better than 0.42 ns and the ΔDOD is about 0.21 ps/s, both are largely improved compared with the S-band VLBI data, which is about 3.41 ns (delay data) and 0.40 ps/s (delay-rate data). Moreover, the short-arc POD tests with ΔDOR data also show excellent results, using ΔDOR and range data with 15 min length arcs is able to improve the accuracy to 140 m, while it was about 250 m using S-band VLBI and range data with 15 min length arcs.

Finally, POD experiments with different lunar gravity models suggest that the 100 degree-order lunar gravity model is enough for the 100 km×100 km lunar orbit, and the SGM100i model that incorporates VLBI data performed better in terms of POD and propagation accuracy compared with other 100 degree models. However, for the 15 km×100 km lunar orbit, higher degree-order up to 165 models can significantly improve the orbit accuracy.

*The authors would like to thank VLBI tracking subsystem at Shanghai Astronomical Observatory for providing the VLBI data used in this paper, and thank Beijing Aerospace Control and Command Center and Beijing Aerospace Control Center for their tremendous support. We would also like to thank Prof. YE ShuHua, QIAN ZhiHan, ZHENG WeiMing, LIU QinHu, LI JinLing, PING JinSong, SHU FengChun, WANG WeiHua, et al. for comments and suggestions. This work was supported by the National Natural Science Foundation of China (Grant Nos. 10703011 and 11073047), the Science and Technology Commission of Shanghai (Grant No. 06DZ22101) and the National High Technology Research and Development Program of China (Grant No. 2010AA122202).*

1 Huang Y, Hu X G, Huang C, et al. Orbit determination of TanCe-1 satellite using VLBI data. Acta Astron Sin, 2006, 47(1): 82–92
2 Huang Y, Hu X G, Zhang X Z, et al. Improvement of orbit determination for geostationary satellites with VLBI tracking. Chin Sci Bull, 2011, 56(26): 2765–2772
3 Cao J F, Huang Y, Hu X G, et al. The effect of lunar gravity field on the low orbit of lunar satellite CE-1. J Astron, 2010, 31(4): 998–1004
4 Cao J F, Huang Y, Hu X G, et al. Mars express tracking and orbit determination trials with Chinese VLBI network. Chin Sci Bull, 2010, 55(32): 3654–3660
5 Luo J T, Chen L, Wu Y J, et al. Progress of testing of a VLBI digital baseband converter. Astron Res Technol, 2010, 7(3): 214–221
6 Li J L, Liu L, Qiao S B. Positioning analysis of observations from X -band monitoring and control system experiments in the Chang'E-2 project. J Geom Sci Technol, 2011, 28(2): 84–87
7 Li J L, Liu L, Zheng W M, et al. The application of positioning reduction in the real-time stage of the Chang'E-2 project. Sci China-Phys Mech Astron, 2011, 41(7): 889–895
8 Zhou X K, Chen Z. Recent progress of ΔDOR technique for deep space navigation and positioning. GNSS World China, 2010, 35(3): 52–57
9 Huang Y. Orbit Determination of the First Chinese Lunar Exploration Spacecraft CE-1. Dissertation for Doctoral Degree. Shanghai: Shanghai Astronomical Observatory, Chinese Academy of Sciences, 2006
10 Liu Y C, Zhang F P, Dong X J. Orbital support to lunar exploration spacecraft (in Chinese). J Spacecr TT & C Technol, 2003, 22(1): 15–19
11 Wang W, Hu X G, Huang Y, et al. Analysis of error sources for trans-lunar spacecraft orbit determination. J Spacecr TT & C Technol, 2005, 24(001): 44–50
12 Huang Y, Hu X G, Dong G L, et al. The effect of wheel off-loading

on the orbit of lunar satellite SMART-1. J Spacecr TT & C Technol, 2007, 26(5): 62–67
13 Liu L, Wang X. An Orbital Dynamics of Lunar Probe. Beijing: National Defence Industry Press, 2006
14 Konopliv A, Asmar S, Carranza E, et al. Recent gravity models as a result of the lunar prospector mission. Icarus, 2001, 150(1): 1–18
15 Yan J G, Ping J S, Li F, et al. Chang'E-1 precision orbit determination and lunar gravity field solution. Adv Space Res, 2010, 46(1): 50–57
16 Chen M, Tang G S, Cao J F, et al. Precision orbit determination of CE-1 lunar satellite. Geom Inform Sci Wuhan Univ, 2011, 36(2): 212– 217
17 Binder A B. Lunar prospector: Overview. Science, 1998, 281: 1475–1476
18 Neumann G A, Mazarico E. Seeing the missing half. Science, 2009, 323: 885–887
19 Carranza E, Konopliv A, Ryne M. Lunar prospector orbit determination uncertainties using the high resolution lunar gravity models. In: Advances in the Astronautical Sciences, AAS/AIAA Astrodynamics Specialist Conference. Girdwood: AAS, 1999. 381–400
20 Goossens S, Matsumoto K, Rowlands D, et al. Orbit determination of the SELENE satellites using multi-satellite data types and evaluation of SELENE gravity field models. J Geod, 2011, 85(8): 487–504
21 Goossens S, Matsumoto K, Liu Q, et al. Lunar gravity field determination using SELENE same-beam differential VLBI tracking data. J Geod, 2010, 85(4): 205–228
22 Liu Q, Kikuchi F, Matsumoto K, et al. Same-beam VLBI observations of SELENE for improving lunar gravity field model. Radio Sci, 2010, 45(2): RS2004
23 Muller P, Sjogren W. Mascons: Lunar mass concentrations. Science, 1968, 161: 680–684
24 Nozette S. The Clementine mission: Past, present, and future. Acta Astron, 1995, 35: 161–169
25 Lemoine F G R, Smith D E, Zuber M T, et al. A 70th degree lunar gravity model (GLGM-2) from Clementine and other tracking data. J geophys res, 1997, 102: 16339–16359
26 Konopliv A, Binder A, Hood L, et al. Improved gravity field of the moon from lunar prospector. Science, 1998, 281: 1476–1480
27 Namiki N, Iwata T, Matsumoto K, et al. Farside gravity field of the moon from four-way DOPPLER measurements of SELENE (kaguya). Science, 2009, 323: 900–905
28 Yan J G, Ping J S, Mastumoto K, et al. Optimization on lunar gravity field model using Chang'E-1 orbital tracking data. Sci China-Phys Mech Astron, 2011, 41(7): 870–878